Check for updates

Purification and Identification of Natural Inhibitors of Protein Arginine Methyltransferases from Plants

Zhengxin Wang,[a] Ling Xiong,[a] Quanbo Xiong[b]

[a]Center for Cancer Research and Therapeutic Development, Department of Biological Sciences, Clark Atlanta University, Atlanta, Georgia, USA
[b]Corteva Agriscience, Indianapolis, Indiana, USA

ABSTRACT Protein arginine methyltransferase (PRMT) enzymes catalyze posttranslational modifications of target proteins and are often upregulated in human cancers. In this study, we purified two chemical compounds from seeds of *Foeniculum vulgare* based on their ability to inhibit the enzymatic activity of PRMT5. These two compounds were identified as Pheophorbide a (PPBa) and Pheophorbide b (PPBb), two breakdown products of chlorophyll. PPBa and PPBb inhibited the enzymatic activity of both Type I and Type II PRMTs with IC$_{50}$ values at sub micromole concentrations, inhibited the arginine methylation of histones in cells, and suppressed proliferation of prostate cancer cells. Molecular docking results predicted that PPBa binds to an allosteric site in the PRMT5 structure with a high affinity (ΔG = -9.0 kcal/mol) via hydrogen bond, ionic, and π-π stacking interactions with amino acid residues in PRMT5. Another group of natural compounds referred to as protoporphyrins and sharing structural similarity with pheophorbide also inhibited the PRMT enzymatic activity. This study is the first report on the PRMT-inhibitory activity of the tetrapyrrole macrocycles and provides useful information regarding the application of these compounds as natural therapeutic reagents for cancer prevention and treatment.

KEYWORDS natural compounds, pheophorbide, protein arginine methyltransferase inhibitors, protoporphyrin, tetrapyrrole macrocycle

The protein arginine methylation is a common posttranslational modification mediated by protein arginine methyltransferases (PRMTs) (1–4). PRMTs catalyze the transfer of methyl groups from S-adenosylmethionine (SAM) onto the arginine residues in target proteins and are classified into three subclasses. Type I PRMTs (PRMT1, PRMT3, PRMT4/CARM1, PRMT6, and PRMT8) generate asymmetric dimethylation of arginine (ADMA-R) residues; Type II PRMTs (PRMT5 and PRMT9) generate symmetric dimethylation of arginine (SDMA-R) residues; Type III PRMT (PRMT7) generates monomethylation of arginine residues. Protein arginine methyltransferases are evolutionarily conserved among eukaryotes (5), and although PRMTs vary in length, each enzyme possesses a dedicated methyltransferase catalytic domain of approximately 310 amino acids essential to the transfer of methyl groups (6).

PRMTs have been implicated in the regulation of gene expression by modification of histones and/or by binding of transcription factors in promoter regions of target genes (7–10). PRMTs have also been reported to affect signal transduction of multiple signaling pathways and to regulate protein subcellular (nucleocytoplasmic) shuttling (11). While PRMT1 is the primary methyltransferase responsible for catalysis of asymmetric dimethylation, PRMT5 is the predominant methyltransferase that generates symmetric dimethylation of arginine residues (7). The loss of PRMT1 in mouse embryonic fibroblasts induces a halt in proliferation (12), and in human embryonic cells PRMT5 is required for proliferation (13). These studies illustrated the importance of PRMT1 and PRMT5 in cellular proliferation. Moreover, it has been reported that cytoplasmic localization of PRMT5 functions to drive cell growth (11). Alternatively, PRMT5 localized to the nucleus has been observed to inhibit cell growth while promoting cell differentiation.

PRMTs tend to be upregulated in cancers (3, 14). However, extensive functional studies are only available for some of them. For example, PRMT1 is overexpressed in nonsmall cell lung carcinoma (15), and PRMT5-mediated increased methylation of EGFR leads to sustained cell proliferation in lung cancer cells (16). Depleting PRMT1 halts the growth of T acute lymphoblastic leukemia by preventing protein synthesis of the MLL1 and MLL4 (17). PRMT5 is expressed in lung cancer, and knockdown of PRMT5 expression inhibited growth of lung cancer cells and lung tumor xenografts (18). PRMTs are prominent therapeutic targets in cancer drug discovery, and great efforts are seen in screening and designing potent and selective PRMT inhibitors (19). Highly potent, selective, and substrate-competitive PRMT inhibitors including MS023 (Type I PRMTs), TP-064 (PRMT4/CARM1), EPZ015666 and others (PRMT5), and EPZ020411 (PRMT6) have been obtained, suggesting that the substrate-binding grooves of PRMTs can be successfully targeted (20, 21). Some of the identified PRMT inhibitors have entered phase I clinical trials (https://clinicaltrials.gov/ct2/home).

Prostate cancer is the second most common cancer in men, and multiple genetic and demographic factors, including age, race, family history, and genetic susceptibility, contribute to the high incidence of prostate cancer (www.cancer.org/cancer/prostate -cancer.html). Radical prostatectomy can cure prostate cancer if it is not spread outside the prostate gland. Men with metastatic prostate cancer receive androgen deprivation therapy (ADT). However, nearly all men with metastatic prostate cancer develop resistance to ADT, a state known as metastatic castration-resistant prostate cancer, which remains a clinically challenging late-stage cancer with no curative treatment options. Dysregulation of PRMTs can be a risk factor for prostate tumorigenesis and prostate cancer progression. Knockout of the gene encoding the PRMT5's partner methylosome protein 50 (MEP50/WDR77) completely blocked prostate tumorigenesis driven by the *Pten* gene deletion in the mouse (22). PRMT1, CARM1, and PRMT5 functioned as candidate epigenetic drivers in prostate cancer progression (10, 23). Therefore, PRMTs are considered to be potential therapeutic targets for prostate cancer treatment.

Chlorophyll and its breakdown products are known for their health benefits, and not only function as colorants, but also possess potential therapeutic properties (24, 25). Pheophorbide a (PPBa) and Pheophorbide b (PBBb) are two products of chlorophyll breakdown, which are formed in algae and higher plants (26). PPBa is composed by a tetrapyrrolic microcycle bearing four methyls, one ethyl, one vinyl, one methoxycarbonyl, and one propionyl as substituents. In PPBb, a formyl group substitutes one methyl group. PPBa is characterized by a strong absorption between 650 and 700 nm, and has been used as a photosensitizer in photodynamic therapy for the treatment of cancer (27). PPBa has been shown to have antiproliferative, antiviral, anti-inflammatory, antioxidant, and antiparasite activity (26). These data show this compound can have a plethora of applications for different human pathologies. The other group of tetrapyrrolic microcycle compounds referred to as protoporphyrin share structural similarity with PPBa and play an important role in living organisms as precursor to other critical compounds like hemoglobins (28).

However, prior to this study, there have been no reports of natural PRMT-inhibitory compounds other than the analogues of the cosubstrate S-adenosylmethionine involved in methyl group transfers. We purified two chemical compounds from seeds of *Foeniculum vulgare* that exhibited the inhibitory activity against both Type I (PRMT1, PRMT3, and PRMT4/CARM1) and Type II (PRMT5) PRMTs. These two compounds were identified as Pheophorbide a (PPBa) and Pheophorbide b (PPBb). PPBa and PPBb showed high potent to inhibit the enzymatic activity of PRMTs with IC$_{50}$ values at the submicromole concentrations. Consistently with the critical role of PRMTs in cell growth, PPBa and PPBb inhibited proliferation of prostate cancer cells. This study opens a new path for cancer prevention and treatment by targeting PRMTs with natural compounds.

RESULTS

Extraction of PRMT5-inhibitory compounds from plants. We began to investigate whether PRMT5-inhibitory compounds could be extracted from plants. An *in vitro*
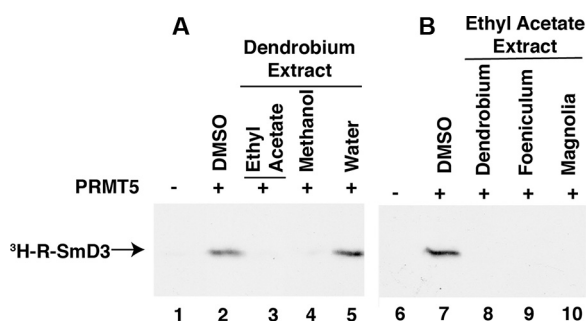
FIG 1 Extraction of PRMT5 inhibitors from plants. An *in vitro* methyltransferase assay was performed with recombinant PRMT5 (0.8 μg, 0.27 μM) and SmD3 (2 μg, 4.4 μM) in the presence of DMSO (5%) (lane 2), the extract (20 μg) of ethyl acetate, methanol, or water from the stem of *Dendrobium* (A), or the ethyl acetate extract (20 μg) from the stem of *Dendrobium*, seed of *Foenlculum*, or leaf of *Magnolia* (B).

methyltransferase assay was used to monitor the activity of PRMTs. The enzymatic activity of PRMT1 and PRMT5 was linear over the 2-h incubation time and were inhibited by their identified small chemical inhibitors (data not shown). Dried stems of *Dendrobium denneanum* were extracted with water, ethanol, methanol, or ethyl acetate at room temperature overnight. Ethyl acetate (lane 3) or methanol (lane 4), but not water (lane 5), extract showed the inhibitory activity against PRMT5 (Fig. 1), suggesting that the PRMT5-inhibitory constituents are not water-soluble. A similar approach was used to extract the PRMT5-inhibitory compounds from other plants, including seeds of *Foeniculum vulgare*, *Ginkgo biloba*, *Pimpinella anium*, and *Zanthoxylum americanum* and leaves of *Magnolia grandiflora*, *Toxicodendron radicans*, and *Thuja arborvitae*. A PRMT5-inhibitory activity was also detected in extracts of the seed of *Foeniculum vulgare* and the leaf of *Magnolia grandiflora* but not in the others. The ethyl acetate extract was then separated by solvent partition with equal volume of water three times to remove water soluble components, and the ethyl acetate fraction was then dried under vacuum. The dried extract was dissolved in methanol and then partitioned with equal volume of hexane for three times to remove lipid soluble components from the extract. The methanol fraction contained a majority of the PRMT5-inhibitory activity and was dried under vacuum. The extracts (20 μg) completely abolished the arginine methylation of SmD3 by PRMT5 (Fig. 1, lanes 8–10).

Purification of PRMT5-inhibitory chemical compounds. The extract of *Dendrobium* was further separated by a HPLC C18 reverse phase chromatography with a linear gradient of acetonitrile-water from 10–100%. Ten major peaks were collected and dried under vacuum. *In vitro* methylation assay indicated the 2 peaks with the retention times of 54 and 56 min contained the PRMT5-inhibitory activity (data not shown), suggesting that *Dendrobium* contains two PRMT5-inhibitory constituents. Electrospray ion mass spectrometry revealed that the two fractions contained two major compounds with the molecular weights of 593.17 and 609.11 daltons, respectively (data not shown). We next switched to the seed of *Foeniculum vulgare* as the initial material for large-scale purification of PRMT5-inhibitory compounds to avoid the limited availability and less quality consistency of dried stems of *Dendrobium denneanum*. The purification scheme is illustrated in Fig. 2. From 1 kg of seeds of *Foeniculum vulgare* we obtained about 7 g of the crude extract. Two PRMT5-inhibitory peaks (F72 and F119) were detected in the fractions from the silica column. The Peak F72 and Peak F119 fractions containing the PRMT5-inhibitory activity were combined separately and further purified through HPLC C18 XTerra and Symetry columns. We obtained 12 mg compound F72 and 7 mg compound F119 from 1 kg of seeds of *Foeniculum vulgare*.

The two purified compounds (F72 and F119) were subject to HPLC-QTOF and high-resolution mass spectrometry (HRMS) analysis. F72 contains a group of analogues with similar molecular weights, and MS/MS analysis revealed that the major peak showed the molecular mass of 592.2765 g/mole and gave the predicted molecular formula $C_{35}H_{36}N_4O_5$. The UV spectrum of F72 showed $\lambda_{max} = 400$ nm. F72 matched well with Pheophorbide a
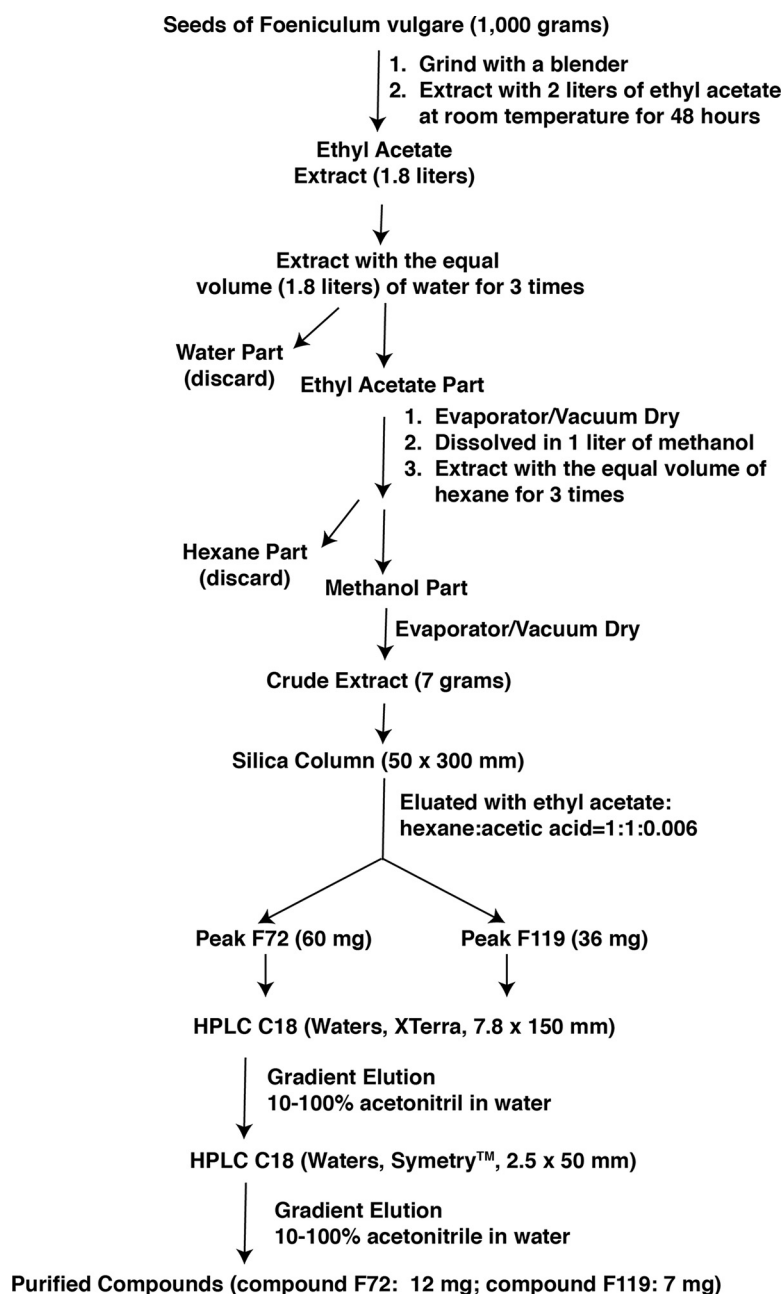
FIG 2 The purification scheme of PRMT5 inhibitors from seeds of *Foeniculum vulgare*.

(PPBa) from searching against the Dictionary of Natural Products (http://dnp.chemnetbase.com). F119 is mainly a compound that gave a molecular mass of 606.2559 and a molecular formula $C_{35}H_{34}N_4O_6$, which matched to Pheophorbide b (PPBb). The UV spectrum of F119 showed $\lambda_{max} = 440$ nm. F72 and the commercial PPBa migrated similarly in the TLC analysis (data not shown). The ^1H and ^{13}C NMR charts (data not shown) of F72 compound also matched that published for PPBa (29–31). It was reported that PPBb could be converted to PPBa by an unknown mechanism (32). We also noticed this conversion during our purification steps. Based on these analyses, we concluded that the PRMT5-inhibitory compounds in *Foeniculum vulgare* are PPBa and PPBb.

PPBa and PPBb inhibited the arginine methyltransferase activity. We then perform *in vitro* methylation assay using the recombinant PRMT1, PRMT3, PRMT4/CARM1, and PRMT5 in the absence or presence of the purified compounds. Both purified
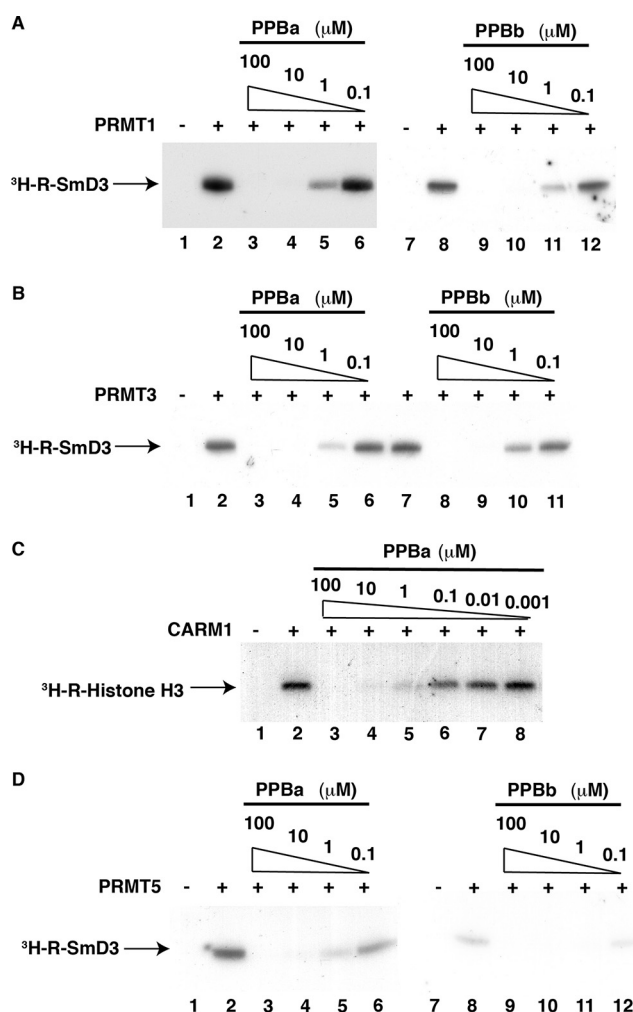
FIG 3 The purified Pheophorbide a (PPBa) and b (PPBb) inhibited the activity of protein arginine methyltransferases. *In vitro* methyltransferase assay was performed with recombinant PRMT1 (0.28 μg) (A), PRMT3 (0.28 μg) (B), PRMT4/CARM1 (0.2 μg) (C), or PRMT5 (0.8 μg) (D) in the presence of DMSO (lane 2) or various concentrations of the purified PPBa or PPBb from *Foeniculum vulgare* as indicated. H^3-SmD3: SmD3 with arginine residues methylated by the tritium-labeled methyl group. H^3-Histone H3: Histone H3 with arginine residues methylated by the tritium-labeled methyl group.

compounds (PPBa and PPBb) inhibited Type I asymmetric (PRMT1, PRMT3, PRMT4/CARM1) (Fig. 3A to C) and Type II symmetric (PRMT5) (Fig. 3D) arginine methyltransferase activity in a dosage-dependent manner. The inhibitory activity of PPBa and PPBb against PRMT1 and PRMT3 was comparable (Table 1). However, PRMT4/CARM1 and PRMT5 are more (3–5-fold) sensitive to PPB than PRMT1 and PRMT3 (Table 1). PPBa purchased from Frontier Scientific (PPBa-F) and Cayman Chemical (PPBa-C) also inhibited the activity of PRMT5 with comparable potency (Fig. 4A, lanes 4–7 versus lane 3). The purified PPBa inhibited PRMT5 activity comparable to the best inhibitor (C2) obtained by screening a small chemical compound library (21) but stronger than the commercial PRMT5 inhibitor (DS-437) and C9 compound (data not shown). PPBa also inhibited the enzymatic activity of the PRMT5-containing complex immunopurified from the FLAG-WDR77 stable cell line (33) (data not shown).

To test whether the purified PPBa could inhibit the activity of protein arginine methyltransferases in cells, we selected histones, the best-known substrates of PRMTs (21), for analysis. Prostate cancer PC3 cells were cultured in the presence of DMSO as a control or with PPBa at various concentrations for 24 h. Histones were then purified and submitted for Western blot analysis with the antibody against the asymmetrical

**TABLE 1** IC$_{50}$ values (μM) of PPBa and PPBb toward PRMTs

Enzyme name	PPBa	PPBb
PRMT1	0.9 ± 0.1	0.7 ± 0.09
PRMT3	1 ± 0.08	0.7 ± 0.1
CARM1	0.3 ± 0.02	
PRMT5	0.2 ± 0.01	0.18 ± 0.02

dimethyl arginine (ADMA-R) or symmetrical dimethyl arginine (SDMA-R) to detect the arginine methylation status in histones. Histones were transferred to NC membrane, stained with Ponceau S to normalize histones loaded on the gel (Fig. 5A, bottom panels), and then immunoblotted with the antibody (Fig. 5A, top panels). The ratio between the band density of the methylated histones (Western blot) and the band density of total histones loaded (Ponceaus staining) is illustrated in Fig. 5B. Consistent with published observations (21), the asymmetrical arginine dimethylation in histones H2A and H4 was detected (Fig. 5A, lane 1), which was inhibited by PPBa in a dosage dependent manner (Fig. 5A, lanes 2–4; 5B). Similarly, the symmetrical arginine dimethylation in histones H3 and H4 was detected (Fig. 5A, lane 5), which was also inhibited by PPBa in a dosage dependent manner (lanes 6–8). Again, PPBa inhibited Type II methyltransferase more potently than Type I methyltransferase (Fig. 5B). In contrast, PPBa did not have any effect on the lysine methylation of histones (Fig. 5C). Thus, the purified PPBa from *Foeniculum vulgare* specifically inhibited the activity of arginine protein methyltransferases *in vitro* as well as in cells.

Purified PRMT-inhibitory compounds suppressed growth of prostate cancer cells. Given the fact that PRMT5 plays a critical role in growth of prostate cancer cells (11, 18), we tested whether the purified PRMT-inhibitory compounds could inhibit growth of prostate cancer PC3 and LNCaP cells. Both PPBa and PPBb inhibited growth of PC3 cells in a concentration-dependent manner with IC$_{50}$ values of 3.5 and 7 μM, respectively (Fig. 6). Similarly, PPBa and PPBb also inhibited growth of LNCaP cells with the IC$_{50}$ values of 4 and 8 μM, respectively (Fig. 7). The purified PRMT-inhibitory compounds from *Dendrobium denneanum* also inhibited growth of LNCaP cells (data not shown). It should be pointed out that certain amounts of Pheophorbide b might be converted to Pheophorbide a in the cultured cells during incubation.
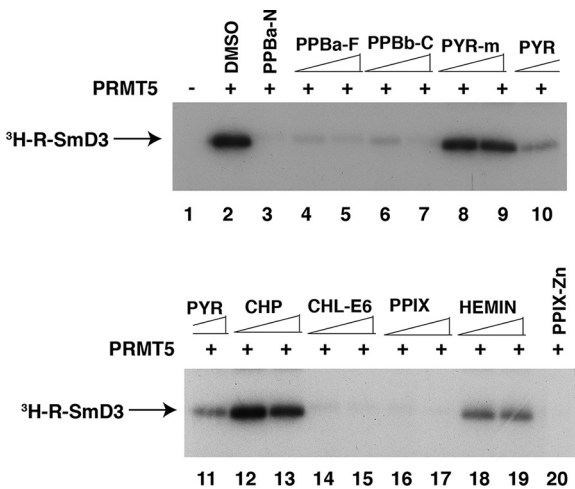
FIG 4 The tetrapyrrole macrocycles inhibited the protein arginine methyltransferase activity of PRMT5. *In vitro* methylation assay was performed with recombinant PRMT5 (0.8 μg) and SmD3 (2 μg) in the presence of DMSO (lane 2), 5 μM purified Pheophorbide a (PPBa-N), or 5 and 10 μM Pheophorbide a purchased from Frontier Scientific (PPBa-F), Pheophorbide a purchased from Cayman Scientific (PPBa-C), Pyropheophorbide a methyl ester (PYR-m), Pyropheophorbide a (PYR), Chlorophyllin sodium copper (CHP), Chlorin e6 (CHL-E6), Protoporphrin IX (PPIX), Hemin, and Protoporphyrin IX Zn (II) (PPIX-Zn) as indicated.
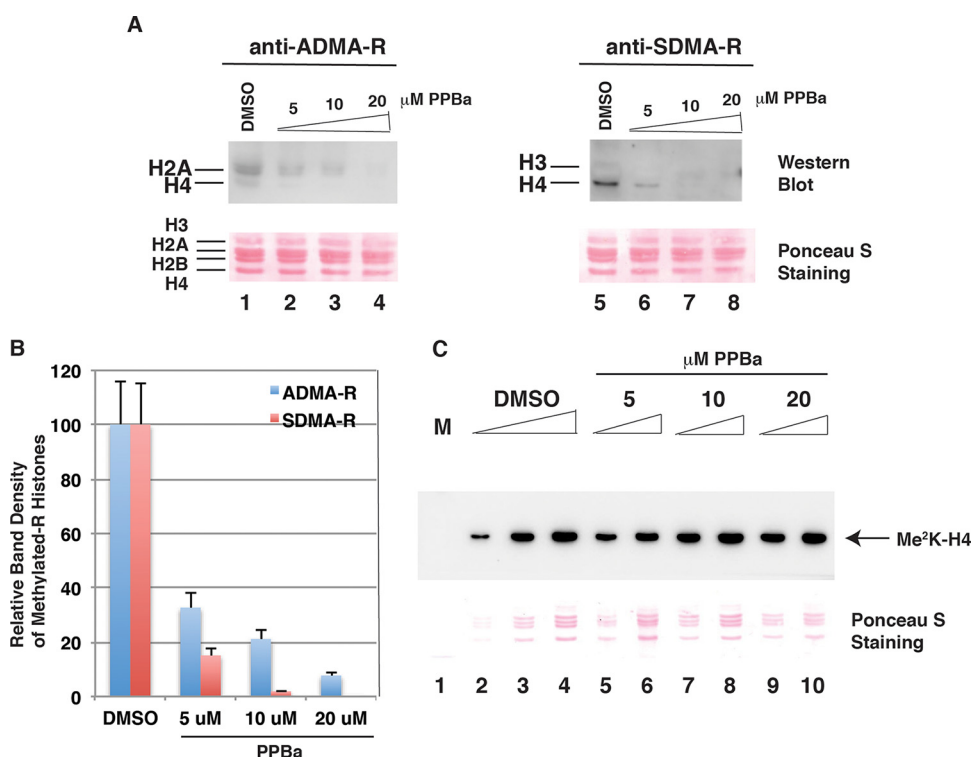
FIG 5 Histone arginine methylation was suppressed by PPBa. (A) Western blot analysis of histones with antibodies against the asymmetric (ADMA-R) or symmetric (SDMA-R) dimethylated arginine. Histones were isolated from PC3 cells grown in the presence of DMSO (lanes 1 and 5) or the purified PPBa at the concentration of 5 (lanes 2, 5), 10 (lanes 3, 7), or 20 (lanes 4, 8) μM for 24 h. The membrane was stained with Ponceau S as the loading control (bottom) before blotting with the antibody (top). (B) Quantitation of the band density of the methylated histones/total histones loaded. The y axis values were normalized using the formula $Y = VALUE/VALUE_{DMSO}*100$. (C) The purified PPBa did not inhibit histone lysine methylation. Western blot analysis of purified histones with antibodies against the lysine methylated histone H4. Histones were isolated from PC3 cells grown in the presence of DMSO (lanes 2–4) or purified PPBa at the concentration of 5 (lanes 5 and 6), 10 (lanes 7 and 8), or 20 (lanes 9 and 10) μM for 2 days. The same samples were stained with Ponceau S to normalize histones loaded (bottom) before blotting with the antibody (top).

Silencing PRMT5 expression resulted in cell cycle arrest in the G1 phase (18). The purified PPBa induced G1 cell cycle arrest and decreased cell populations in the S phase (data not shown), consistent with the fact that the purified PPBa inhibited the PRMT5 activity. It was noticed that the purified PPBa also decreased the cell population in the G2 phase. The purified PPBa did not induce apoptosis because it did not affect the subG1 cell populations.

We previously showed that the enzymatic activity of PRMT5 is required for cellular proliferation (11). The BrdU incorporation assay was used to label proliferative cells. Eight-one percent PC3 cells were BrdU-positive when cells were cultured in the presence of DMSO (Fig. 8). In contrast, the treatment of PC3 cells with the purified PPBa significantly decreased cell populations of BrdU-positive cells in a dosage-dependent manner (Fig. 8), suggesting that the purified PPBa inhibited cellular proliferation.

The tetrapyrrole macrocycles inhibited the PRMT5 enzymatic activity. The PPBa was docked against PRMT5 using AutoDock Vina (34). The best-scored conformation was selected by considering the lowest binding energy between the protein and the compound. The best-selected pose of PRMT5-PPBa docked complex (the binding energy: −9.0 kcal/mol) predicted by AutoDock Vina is showed in Fig. 9A. PPBa sits in a pocket formed by α-helix 12 (amino acids [aa] 296-302), α-helix 21 (aa 569-571), β-sheet 19 (aa 509-511), α-helix TF (a. 215-225), and α-helix TG (aa 248-257) in PRMT5 (Fig. 9A and B). The carboxylic acid [C(17^3)OOH] in PPBa forms three hydrogen bond interactions with E305 and A301 amino acid residues in PRMT5 (Fig. 9C, panel a). Ionization of this carboxylic acid would generate the slightly different interactions
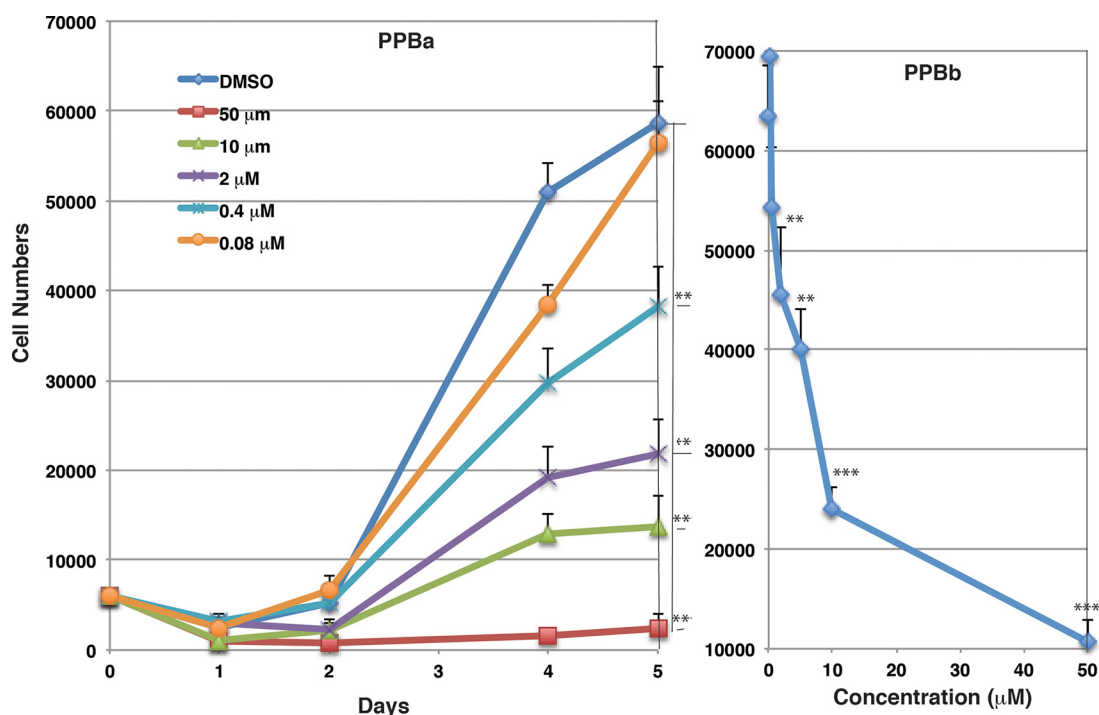
FIG 6 The purified PPBa suppressed prostate cancer cell growth. PC3 cells were grown in the presence of DMSO or purified PPBa (left) or PPBb (right) at various concentrations, and cell numbers were counted.

between PPBa and PRMT5 (Fig. 9C, panel b). These interactions include a hydrogen bond between the carboxylic acid and E305 and an ionic interaction between the ionized carboxylic acid and K302. The hydroxyl group {C(13^1)-OH, the enol form of the ketone group [C(13^1) = O]} forms hydrogen bonds with both Y297 and R505 amino acid residues in PRMT5. The phenyl ring of amino acid F509 forms the π-π stacking interaction with the PPBa pyrrole ring B (Fig. 9C). There are also hydrophobic interactions between PPBa with the hydrophobic residues in the pocket of PRMT5. These would
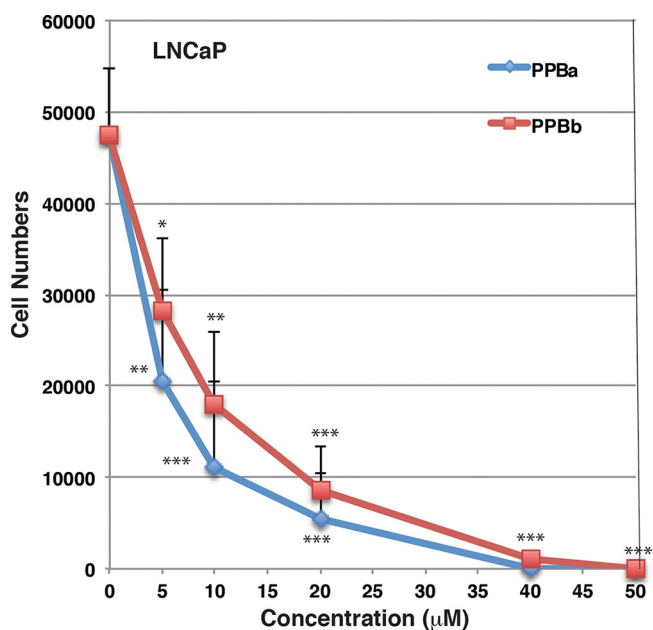
FIG 7 Purified Pheophorbide a (PPBa) and b (PPBb) suppressed prostate cancer cell growth. LNCaP cells were grown in the presence of DMSO or purified PPBa (blue) or PPBb (red) at various concentrations for 3 days, and cell numbers were counted.
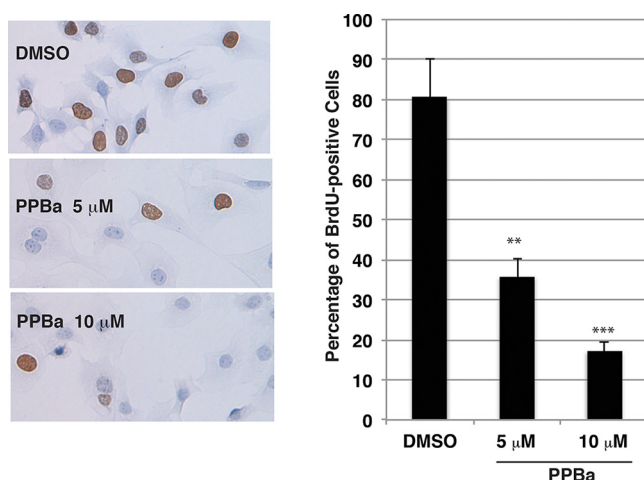
FIG 8 The purified PPBa inhibited cellular proliferation. PC3 were grown in the presence of DMSO (0.1%) (top panel), or PPBa at 5 (middle pane) or 10 (bottom panel) μM for 3 days and labeled with BrdU for 2 h. Cells were stained with anti-BrdU antibody (brown) (left). Right, quantitation of BrdU-positive cells.

suggest a strong interaction between PPBa and PRMT5, which is consistent with a high binding affinity ($\Delta G = -9.0$ kcal/mol) indicated by the molecule docking and the low IC_{50} in the inhibition of the PRMT5 enzymatic activity.

PPBa was similarly docked against PRMT1 and other PRMTs. The best-selected pose of PRMT1-PPBa docked complex (the binding energy: -8.0 kcal/mol) predicted by AutoDock Vina is shown in Fig. 10. PPBa was docked on the substrate-binding site that is closed to the SAM-binding site (Fig. 10A and B). The docking analysis demonstrated that PPBa interacted with PRMT1 via multiple hydrogen bonds formed with I272, R280, and S284 (Fig. 10C). The less binding energy of PPBa to PRMT1 than PRMT5 is consistent with its less efficacy in the inhibition of PRMT1 than PRMT5 enzymatic activity in the methylation assay (Fig. 3; Table 1). PPBa was also docked on the substrate-binding site of the other type PRMTs (PRMT3, PRMT4/CARM1, PRMT6, PRMT7, and PRMT8) with binding energy from 7.0 to 8.0 kcal/mol, with the exception of the PRMT4/CARM1-PPBa docked complex, which has the highest binding energy at -9.9 kcal/mol, consistent with the fact that PPBa is a more potent inhibitor for PRMT5/CARM1 (Fig. 3).

We purchased 4 analogues (Pyropheophorbide a, Pyropheophorbide a methyl ester, Chlorin e6, and Clorophyllin sodium copper salt) of PPBa and our protoporphyrin compounds [Protoporphrin IX, Protoporphrin IX Zn (II), and Hemin] for the analysis. We tested their ability to inhibit the PRMT5 enzymatic activity in the methylation assay (Fig. 4). Chlorin e6 and PPIX inhibited PRMT5 even better than PPBa, and the other compounds are less effective than PPBa. Cu (Fig. 4A, lanes 12 and 13) and Fe (lanes 18 and 19) ions but not the Zn (lane 20) ion in the ring decreased the compounds' PRMT5 inhibitory activity. The ester formation of the carboxylic acid in Pyropheophorbide a methyl ester significantly (by 2-fold) decreased the compound's inhibitory activity (Fig. 4A, lanes 8 and 9 versus lanes 10 and 11), which is consistent with the docking result that the carboxylic acid is involved in the formation of hydrogen bonds or ionic interaction with PRMT5 (Fig. 9C). These compounds also inhibited the PRMT1 activity similarly. These results suggested that tetrapyrrole macrocycles with marked aromatic character and broad utilizations (35–37) have the ability to inhibit the enzymatic activity of protein arginine methyltransferases.

DISCUSSION

While increasing numbers of PRMT inhibitors have been identified (19), there have been no reports of natural PRMT-inhibitory compounds from plants. In the present study, we purified and identified, for the first time, two natural compounds (PPBa and PPBb) that inhibited the activity of both Type 1 and Type II protein arginine
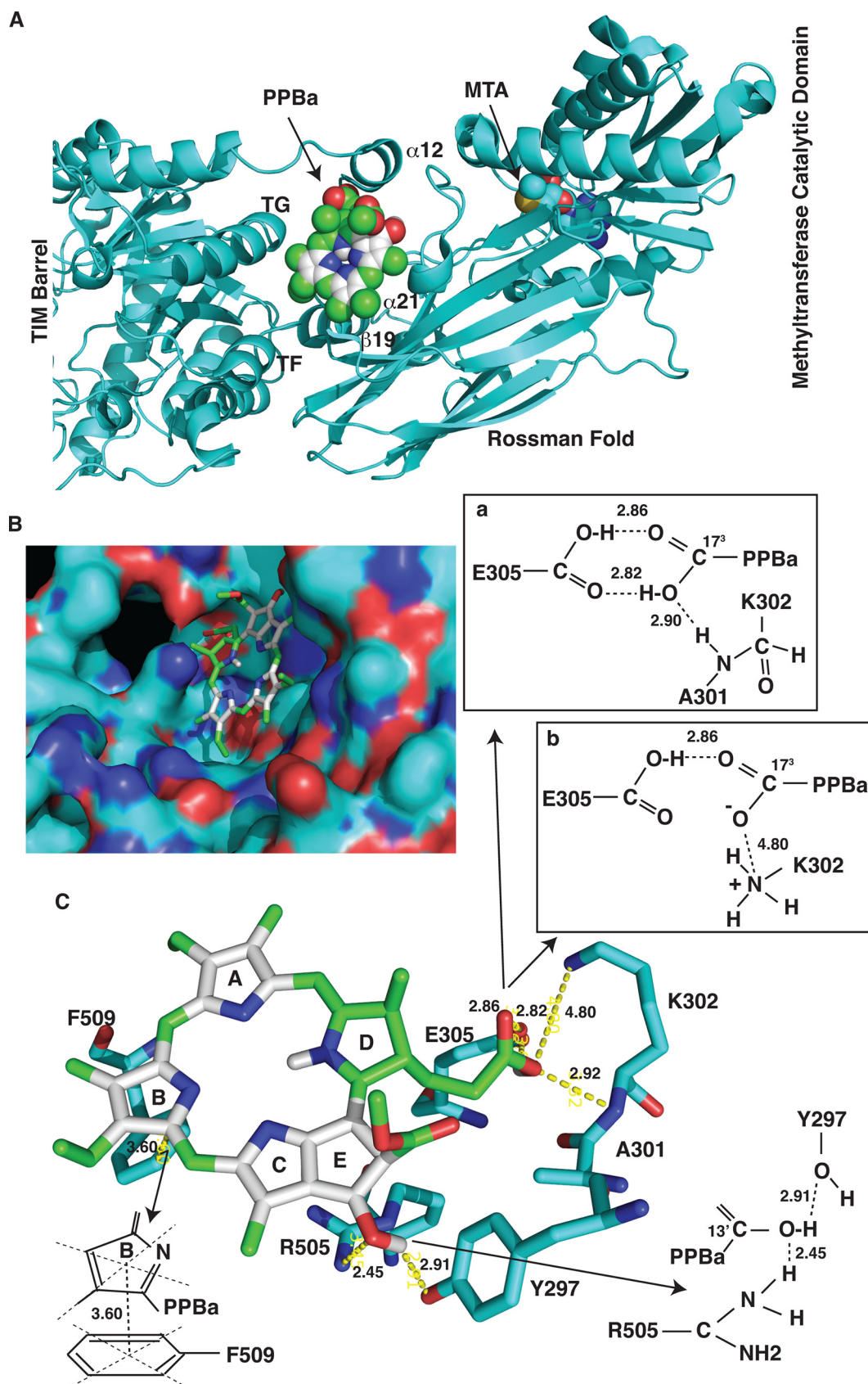
FIG 9 Docking studies predict PPBa binds PRMT5 at a novel site. (A) The output of AutoDock showing the binding site of the PRMT5 protein with PPBa. The SAM analogue, 5′-Deoxy-5′-methylthioadenosine (MTA), was also included in the

methyltransferases *in vitro* as well as in cells. The purified PPBa and PPBb inhibited growth of prostate cancer cells, which was correlated well with their inhibitory activity on the protein arginine methyltransferases.

PPBa and PPBb function as potent PRMT inhibitors. The PRMT5-inhibitory constituents could be extracted from 3 plants among 8 plants tested. Two PRMT5-inhibitory compounds were purified to homogeneity from two plants and further identified as PPBa and PPBb based on the followings. First, the high-resolution mass spectrometry analysis indicated two purified compounds are PPBa and PPBb. Second, NMR charts of the purified compound F72 matched to those published for PPBa (29–31). Third, we observed the conversion of compound F119 to compound F72 during purification steps. This observation fits with the documented fact that PPBb could be transformed to PPBa. Fourth, PPBa purchased from two commercial resources showed the similar inhibitory activity to PRMT5. The commercial PPBa was prepared by the semisynthesis (30), which is different from our preparation procedures. PPBa and PPBb also inhibited the other PRMTs. In addition, we found that some of protoporphyrins also strongly inhibited the PRMT5 activity. Humans convert chlorophylls into Pheophytin, Pyropheophytin, or Pheophorbide during the digestion of vegetables (24). The next important questions are why some plants produce PPBa and PPBb and whether they have physiological roles in the plant (25). It is also interesting to know how these compounds could affect the physiology of human beings by serving as PRMT inhibitors.

PPBa was predicted to bind to an allosteric site in PRMT5. Most of identified highly potent and selective PRMT inhibitors bind to the substrate-binding grooves of PRMTs (19). A PRMT3 inhibitor was discovered to bind to the interface of the two PRMT3 subunits and functioned as an allosteric inhibitor of PRMT3 (38). By performing molecular docking analysis, we found PPBa binding to the substrate-binding groove of Type I PRMT structures but to an allosteric site in the Type II PRMT (PRMT5) structure. The site is not localized at the methyltransferase catalytic domain of PRMT5, but rather at the linker region that bridges the catalytic domain with the N-terminal TIM barrel. The support for the binding model was provided by the compound Pyropheophorbide a methyl ester in which the carboxylic acid, which plays an import role in the PRMT5 interaction, is substituted by a methyl ester. The substitution lost about half of the inhibitory activity toward the PRMT5 methyltransferase. The phosphorylation of several tyrosine residues in the α-helix 12 by the Jak2 kinase greatly impaired the PRMT5 enzymatic activity (39), suggesting that this region plays an important role in the regulation of the PRMT5 activity. Since PPBa is binding to an allosteric site, it would be interesting to know whether PPBa and previously identified PRMT5 inhibitors (binding to the catalytic domain) could function synergistically to inhibit the PRMT5 activity. However, we failed to observe such synergism. The molecular docking result shows that PPBa makes tight contacts with amino acid residues Tyr297 and Glu298 in the α-helix 12 (Fig. 11). When superposing the PRMT5 structure (5fa5) including histone H4 (1-20) and 5′-Deoxy-5′-Methylthioadenosine on the PRMT5 structure (6k1s) including a substrate-binding inhibitor, we found that the helix 12 moved inside the pocket, resulting in upward movement of the Tyr297 by 0.98 Å and inside movement of oxygen atoms (OE1 and OE2) in the side chain of Glu298 by 3.13 and 1.72 Å (Fig. 10B). The structural changes in the Helix 12 would prevent PPBa-binding to the pocket. Indeed, molecular docking showed that PPBa failed to bind to the pocket in the inhibitor binding-PRMT5 structure. The similar results were also obtained with the inhibitor EPZ015666-binding PRMT5 (4x61).

Anti-cancer activity of PPBa. PRMTs are upregulated in various cancers (3, 14), and PRMT-inhibitors represent a promising group of compounds for cancer treatment (19–21).

FIG 9 Legend (Continued)
structure. (B) PPBa sits in the pocket formed by α12, α 21, β19, TF, and TG in the PRMT5 structure. (C) The output of AutoDock Vina showing the binding residues of the PRMT5 protein with PPBa. Inserts, 2D diagram showing the types of contacts formed between PRMT5 and PPBa. The dotted lines indicate H-bond or ionic interactions between PPBa and PRMT5. The values adjacent to the dotted lines indicate their distance.
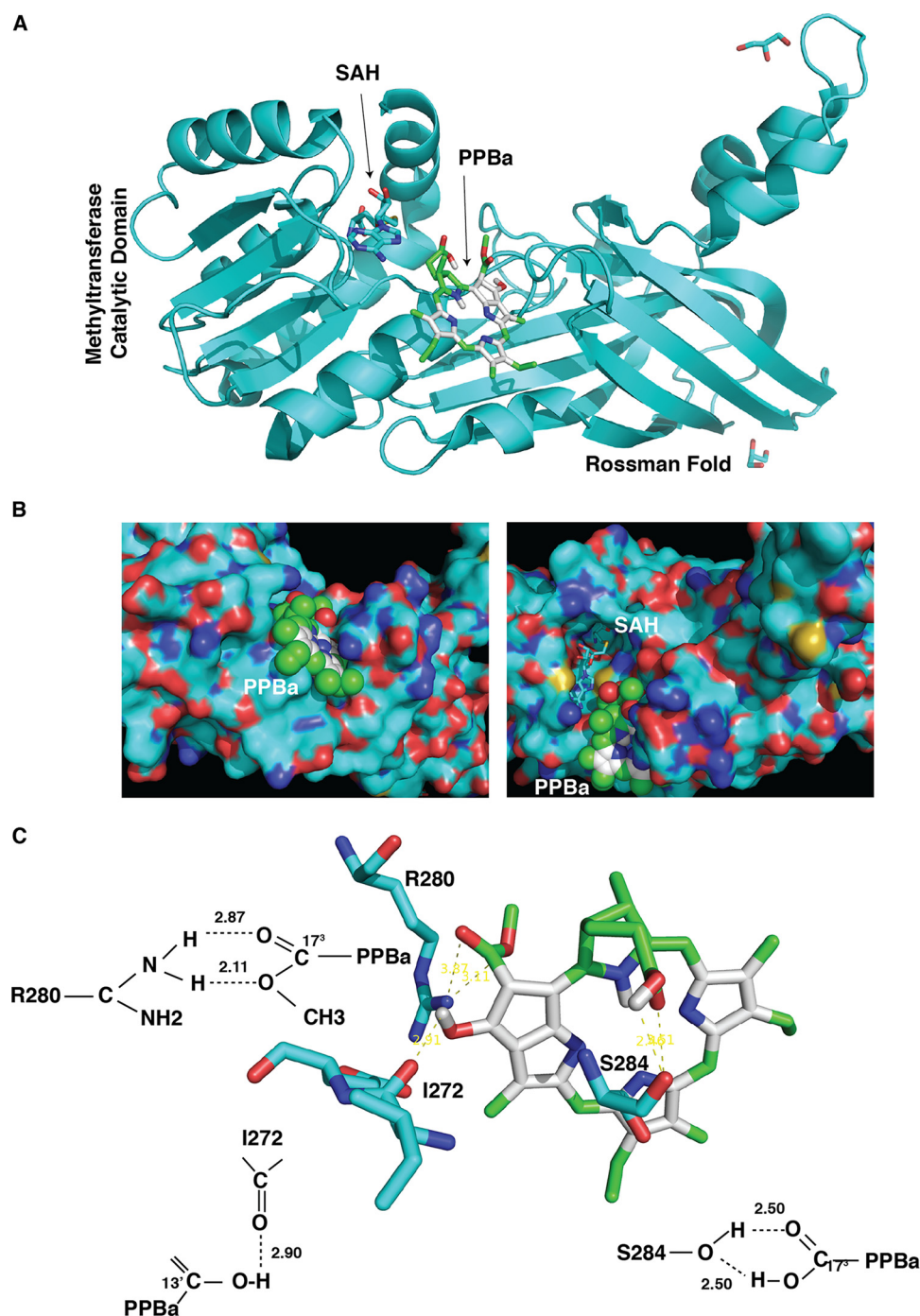
FIG 10 Docking studies predict PPBa binds PRMT1 at the substrate-binding site. (A) The output of AutoDock showing the binding site of the PRMT1 protein with PPBa. (B) PPBa sits in the cavern of the PRMT1 structure. (C) The output of AutoDock Vina showing the binding site residues of PRMT1 protein with PPBa. 2D diagrams showing the types of contacts formed between PRMT1 and PPBa. The dotted lines indicate H-bond interactions between PPBa and PRMT1. The values adjacent to the dotted lines indicate their distance.

For example, PRMT1 was reported to be upregulated in breast cancer (40), renal cell carcinoma (41), and colon cancer (42) to promote proliferation and transformation of cancer cells. PRMT5 has been shown to be upregulated in a number of different cancers and play an essential role in growth of various cancer cells (43, 44). Consistently with these observations, PRMT5 inhibitors suppressed growth of lymphoma, acute myeloid leukemia, and mantle cell lymphoma (MCL) cells in tissue culture (45–47). More recently, EPZ015666

A
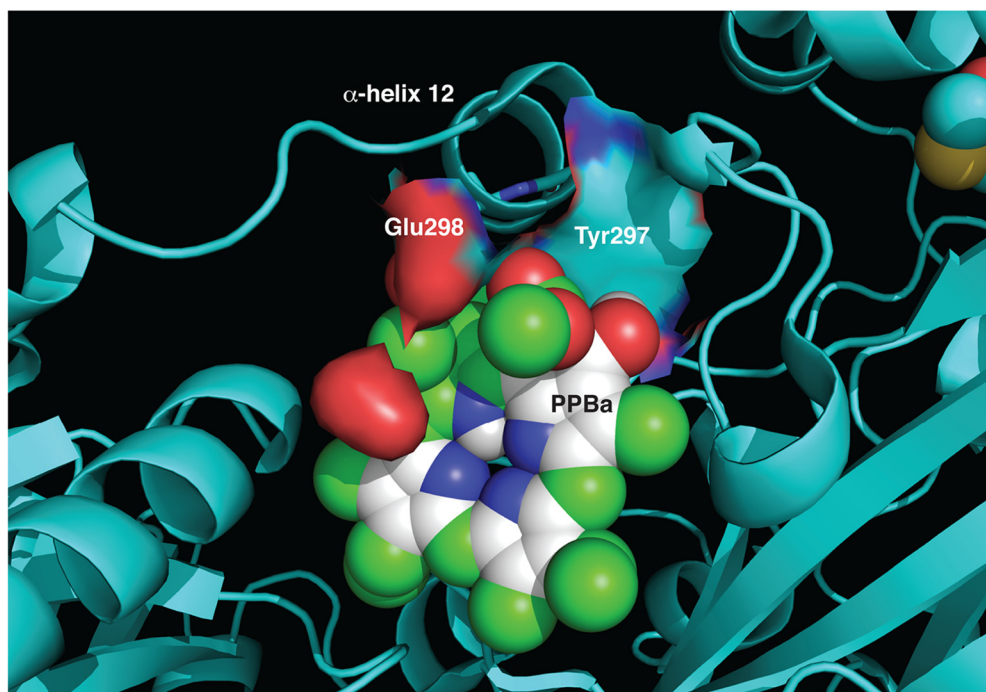
B
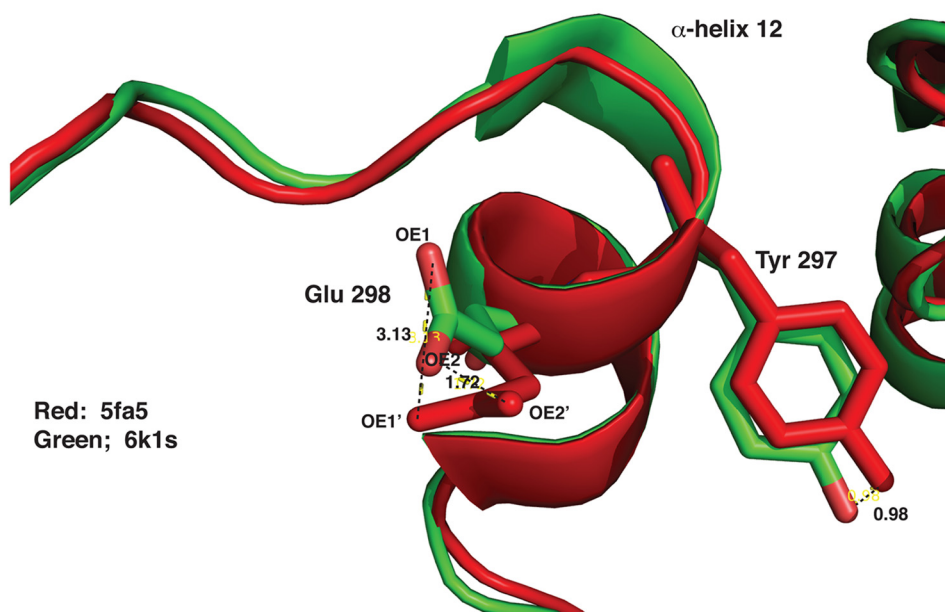
FIG 11 Docking studies predict the inhibitor binding to the substrate-binding site prevents the binding of PPBa to PRMT5. (A) PPBa has tight contacts with amino acid residues Glu298 and Tyr297 in the α-helix 12. The diagram shows the surface contacts of Glu298 and Tyr297 with PPBa. (B) The α-helix shifts its position upon the biding of the inhibitor to the substrate-binding site of PRMT5. The overlap of the PRMT5 structure that binds to the substrate (5fa5, red) with the PRMT5 structure that binds to the inhibitor (6k1s, green). The values adjacent to the dotted lines indicate their distances shifted.

demonstrated antitumor activity in multiple MCL xenograft models (47). Previous studies using RNA interference technologies revealed an essential role of PRMT5 in growth of lung cancer cells and lung tumor xenografts (18). We have shown in this report that identified PRMT5 inhibitors inhibited growth of prostate cancer cells. This inhibitory effect on cell growth is through the arrest of cells in the G1 phase of the cell cycle, not through

induction of apoptosis, which is consistent with the documented role of PRMT5 in the control of cellular proliferation (18, 48). PPBa demonstrated the high inhibitory activity toward PRMT5 with the IC_{50} at 0.2 μM, which is comparable with PRMT5-specific inhibitors recently identified by screening chemical libraries (45–47, 49). In addition, it also inhibited the PRMT1 enzymatic activity. Recently, it was shown that PRMT1 loss sensitized cells to PRMT5 inhibitors (50) and, therefore, the dual activity of PPBa might have an additional advantage than the more selective PRMT5 inhibitors in cancer treatment. Alteration of PRMT4/CARM1, mostly upregulation, was frequently reported in various types of human cancers, which appears to promote cancer initiation, progression, and metastasis (14). These natural PRMT inhibitors reported here could also be used to target PRMT4/CARM1 for cancer treatment.

Pheophorbide a is a photosensitizer that has been used for photodynamic therapy (26). Upon administration of light (660 nm), Pheophorbide a can induce significant antiproliferative effects through reactive oxygen species (ROS) in several human cancer cell lines (27). We found that Pheophorbide a as a photosensitizer inhibited cell proliferation at much lower concentrations (IC_{50}: 0.2 μM, 660 nm, 4 min at 2.8 J/cm^2) but did not through PRMTs. In contrast, the PRMTs-mediated inhibitory effect on cell proliferation by Pheophorbide a needed higher concentrations (IC_{50}: 3.5–7 μM). All experiments performed here avoided exposure to light, and Pheophorbide a inhibits cell proliferation most likely through PRMTs without light. The tetrapyrroles chelate metals in cells, which could affect cellular functions (51). This metal-chelating activity of PPBa and PPBb might also contribute to their observed cell growth inhibition.

Conclusions. The present study clearly demonstrated that the natural products PPBa and PPBb inhibit the PRMT activity. Given that PRMTs play an essential role in growth of various cancer cells, the identified natural PRMT-inhibitory compounds could serve as agents for cancer prevention and treatment. One of the major drawbacks for anti-cancer agents is the unwanted side effects. Given the fact that PPBa and PPBb can be consumed in vegetables and have beneficial effects to human beings, the adverse effects of these PRMT-inhibitory compounds might not be significant. Future studies will be to test them for their therapeutic treatment of cancers.

MATERIALS AND METHODS

Chemicals. Pheophorbide a (#Pha-592), Peopheophorbide a (#PPa), and Propheophorbide a methyl ester (#MPPa) were purchased from Frontier Chemicals. Pheophorbide a (#16072) and Chlorin e6 (#21684) were purchase from Cayman Chemicals. Chlorophyllin sodium copper salt (#C6003), Protoporphyrin IX (#P8293), Protoporphyrin IX zinc (II) (#282820), Hemin (#51280), EPZ015666 (#SML1421), and DS-437 (#SML1516) were purchased from Sigma-Aldrich. GSK3368715 (#S8858) was purchased from Selleckchem.

Extraction and isolation. Dried seeds of *Foeniculum vulgare* were purchased from Great Wall Supermarket (Duluth, GA). The purification procedure is illustrated in Fig. 2. The seeds were ground to powder and extracted with ethyl acetate at the room temperature. The extract was then partitioned with an equal volume of water three times and then dried. The dry extract was dissolved in methanol and then partitioned with an equal volume of hexane three times. The methanol fraction contained the majority of the PRMT5-inhibitory activity and was dried. The dried material was subjected to a Silica (Sorbent Technologies, Inc.) column (5 mm $\times$ 300 mm), and the column was eluted with ethyl acetate:hexane:acetic acid (1:1:0.006). Two peaks (F72 and F119) with the PRMT5-inhibitory activity were pooled separately and dried. The dried materials were dissolved in 40% acetonitrile (vol/vol) in water and subjected to an HPLC C-18 column (Waters, Xterra 7.8 $\times$ 150 mm). The column was eluated with a linear gradient of acetonitrile/water from 10–100% (vol/vol) in 60 min. Two compounds with the PRMT5-inhibitory activity were dried under vacuum and further purified by an HPLC C18 column (Waters, Symetry, 2.5 $\times$ 50 mm).

Assay for the PRMT-inhibitory activity. Human PRMT1, PRMT3, PRMT5, and human small nuclear ribonucleoprotein SmD3 were expressed in bacteria and purified as previously reported (21). The recombinant PRMT4/CARM1 was purchased from Abcam (ab196401). The C-terminal region of the SmD3 protein contains multiple GR sequences that can be methylated by PRMTs. The SmD3 protein was used as a substrate for the methylation assay. The reaction mixture (40 μl) contained recombinant SmD3 (2 μg, 4.4 μM) or purified histones (0.6 μg) (33), H^3-SAM (1 μCi, 10 μM), recombinant PRMT1 (0.28 μg, 0.17 μM), PRMT3 (0.28 μg, 0.11 μM), PRMT4/CARM1 (0.2 μg, 0.07 μM), or PRMT5 (0.8 μg, 0.27 μM), and the chromatographic fraction or chemical compound dissolved in DMSO (2 μl, 5%) in the reaction buffer (50 mM Tris-HCl, pH 7.5, 1 mM EDTA, 1 mM EGTA, 10 mM DTT) and was incubated at 30°C for 2 h. The reactions were terminated by the addition of 10 μL of 5$\times$ sodium dodecyl sulfate (SDS) sample buffer and were separated by 15% SDS-polyacrylamide gel electrophoresis (SDS-PAGE). The gel was fixed with 40% methanol and 10% acetic acid for 10 min and incubated in Amplify (GE Healthcare) for 30 min. The gel was dried under vacuum and exposed to an X-ray film. Bands were subjected to densitometry (Bio-Rad) for quantitation. To calculate IC_{50}, compound

concentrations (x_1, x_2, . . ., x_n) and methylation inhibition (y_1, y_2, . . ., y_n) were plotted (x-y) and linear regression was performed. IC_{50} value was then calculated using the fitted line, i.e., $Y = a*X+B$, $IC_{50} = (0.5–b)/a$.

Mass spectrometry analysis. Two purified compounds (F72 and F119) were submitted for the high-resolution mass spectrometry (HRMS) analysis. The Agilent 1290 HPLC system was connected to a diode array detector followed by an Agilent 6545 quadruple time of flight mass spectrometry (Agilent Technologies, Santa Clara, CA) equipped with dual electrospray electro spray ionization interface. The LC/QTOF-MS analysis was performed on a reversed-phase Hypersil Gold-C18 analytical column of 2.1 × 50 mm and 1.9 μm particle size (Thermo Fisher). An aliquot (1 μL) of sample solution in acetonitrile was injected in each run. The mobile phase consisted of 0.1% formic acid in both water (A) and acetonitrile (B). The chromatography was run at isocratic 60% B at 0.4 mL/min. For HRMS, the following operation parameters were used in a positive mode: capillary voltage, 3,500 V; nozzle voltage 1,000 V; gas temperature 300℃; drying gas 10 L/min; nebulizer pressure, 35 psig; sheath gas temperature, 350℃; sheath gas flow 12 L/min. For untargeted MS/MS analysis, a formula of 8 × mz/100 + 4 was used to determine collision energy for fragmentation. Molecular formula was predicted using the Agilent MassHunter Qualitative Analysis software based on the accurate mass of adduct complex, isotope space, and relative intensity. The samples were also sent to the Mass Spectrometry Facility at Georgia State University for the routine mass spectrometry analysis to determine the purity of HPLC peaks.

NMR analysis. The purified compound F71 (12 mg) was dissolved in 0.8 mL of DMSO-d6, and the solution was placed in a 5-mm NMR tube. The sample was submitted to the analysis using a 500 MHz NMR spectrometer (Brucker Advance III) at the NMR Facility at Clark Atlanta University. ^{1}H and ^{13}C NMR spectrums were recorded. Chemical shifts were given in parts per million relative to tetramethylsilane, using the DMSO-d6 resonance at 2.50 (^{1}H) and 39.5 (^{13}C) ppm as the internal standard. The assignments of [1]H- and ^{13}C-signals of the compound F72 (Pheophorbide a) were made on the basis of reported data (29–31).

Cell culture and compound treatment. LNCaP and PC3 prostate cancer cell lines obtained from the American Type Culture Collection (ATCC) were maintained in RPMI 1640 medium supplemented with 10% fetal bovine serum (FBS; Atlanta Biologicals) and 100 mM penicillin/streptomycin in Corning T-75 flasks. Cells were incubated at 37℃ in humidified atmospheric conditions of 5% CO_2. For cell growth assay, LNCaP and PC3 cells were seeded into 24-well plates at 1.0×10^4 and 6×10^3 cells per well, respectively. On the following day, culture medium was replaced with RPMI 1640 supplemented with 2% FBS in the presence of DMSO (0.1%) or the compound at the concentrations as indicated. Cells were grown for various times and were harvested for cell counting or various assays (Western blot, BrdU incorporation, and cell cycle analysis). To calculate IC_{50}, compound concentrations (x_1, x_2, . . ., x_n) and growth inhibition (y_1, y_2, . . ., y_n) were plotted (x-y) and linear regression was performed. IC_{50} value was then calculated using the fitted line, i.e., $Y = a*X+B$, $IC_{50} = (0.5–b)/a$. For BrdU incorporation assay, PC3 cells were seeded onto coverslips in 6 well-plates at densities of 2.5×10^6 cells per well. After 24 h, cells were treated with PPBa for 3 days and cultured in the media containing BrdU (10 μM) (Beckton Dickinson Biosciences, 247580) for 2 h. The cells were immunostained with anti-BrdU antibody (Beckton Dickinson Biosciences) as published previously (18). For cell cycle analysis, PC3 cells were seeded into 100 mm VWR Tissue Culture Dishes (10062-880) at 2.4×10^5 cells per dish and permitted to attach overnight. On the following day, cells were washed using PBS and treated with PPBa for 3 days. Cells were harvested, washed using PBS, and fixed overnight in 70% ethanol. Cells were stained with propidium iodide solution (15 μM) and submitted for cell cycle analysis using the Accuri C6 Flow Cytometer and analyzed with the FlowJo software.

Protein isolation and quantification. Whole cell protein lysates were prepared using the Protein Lysis Buffer (Promega, E194A), supplemented with Phosphatase Inhibitor Cocktail (Santa Cruz, 45044) and Protease Inhibitor Cocktail (Active Motif, 100510). Histones were purified from cells as reported (21). Briefly, cells were harvested, washed with PBS (1 mL), and lysed with the 1 × Passive Lysis Buffer (0.5 mL). After centrifugation (12,00 rpm for 10 min at 4℃), the cell pellet was washed with 1 × Passive Lysis Buffer (0.5 mL) and extracted using 0.2 M H_2SO_4 (0.1 mL) and then precipitated with acetone (0.4 mL, −20℃). Proteins were pelleted by centrifugation at 12,000 rpm for 10 min at 4℃, and the pellet was washed with acetone and air-dried. Protein concentrations were measured by using the Protein Assay Dye Reagent Concentrate (Bio-Rad, 500-0006) with Bovine Serum Albumin (BSA) (New England BioLabs, B9001S) as the standard. Standards and samples were measured in triplicate with each coefficient R value ≥ 0.998.

Western blot analysis and antibodies. Proteins were separated by SDS-PAGE and transferred to a nitrocellulose membrane (Whatman BA83). The membrane was blocked with 3% nonfat milk (Santa Cruz 2324) for 30 min and incubated in a primary antibody for 2 h. and then the secondary antibody labeled with HRP for 1.5 h. The membrane was washed 4 times, and the protein band was visualized using an enhanced chemiluminescence substrate (PerkinElmer, NEL103001EA). The anti-PRMT5 antibody was purchased from Fisher Scientific (PA5-78323). Anti-dimethyl-arginine, symmetric (SYM10) polyclonal rabbit antibody (07-412) and anti-dimethyl-arginine asymmetric antibody (ab413) were obtained from EMD Millipore and Cell Signaling, respectively. Anti-β-Actin (A2103) polyclonal rabbit antibody was obtained from Sigma-Aldrich.

Molecule docking. Molecule docking was performed with crystal structures of human PRMT5 (5fa5) and PRMT1 (6nt2) using AutoDock Vina software (34) (http://vina.scripps.edu/). For PRMT5 docking, the grid box size was set at 50, 88, and 56 Å for x, y, and z, respectively. The grid center was set at −28.837, −83.973, and −14.841 Å for x, y, and z, respectively. For PRMT1 docking, the grid box size was set at 46, 66, and 48 Å for x, y, and z, respectively. The grid center was set at 2.746, 33.006, and 18.53 Å for x, y, and z, respectively. The spacing between the grid points was 1.0 Å. The interactions were analyzed by visualizing software PyMOL (https://pymol.org/2/).

ACKNOWLEDGMENTS

REFERENCES

1. Blanc RS, Richard S. 2017. Arginine methylation: the coming of age. Mol Cell 65:8–24. https://doi.org/10.1016/j.molcel.2016.11.003.
2. Peng C, Wong CC. 2017. The story of protein arginine methylation: characterization, regulation, and function. Expert Rev Proteomics 14:157–170. https://doi.org/10.1080/14789450.2017.1275573.
3. Poulard C, Corbo L, Le Romancer M. 2016. Protein arginine methylation/demethylation and cancer. Oncotarget 7:67532–67550. https://doi.org/10.18632/oncotarget.11376.
4. Bedford MT. 2006. The family of protein arginine metkyltransferases, p 31–50. In Clarke SG, Tamanoi F (ed), The enzymes. Elsevier, Amsterdam, The Netherlands. https://doi.org/10.1016/S1874-6047(06)80004-1.
5. Wang YC, Li C. 2012. Evolutionarily conserved protein arginine methyltransferases in non-mammalian animal systems. FEBS J 279:932–945. https://doi.org/10.1111/j.1742-4658.2012.08490.x.
6. Zhang X, Zhou L, Cheng X. 2000. Crystal structure of the conserved core of protein arginine methyltransferase PRMT3. EMBO J 19:3509–3519. https://doi.org/10.1093/emboj/19.14.3509.
7. Bedford MT, Clarke SG. 2009. Protein arginine methylation in mammals: who, what, and why. Mol Cell 33:1–13. https://doi.org/10.1016/j.molcel.2008.12.013.
8. Pal S, Vishwanath SN, Erdjument-Bromage H, Tempst P, Sif S. 2004. Human SWI/SNF-associated PRMT5 methylates histone H3 arginine 8 and negatively regulates expression of ST7 and NM23 tumor suppressor genes. Mol Cell Biol 24:9630–9645. https://doi.org/10.1128/MCB.24.21.9630-9645.2004.
9. Krause CD, Yang ZH, Kim YS, Lee JH, Cook JR, Pestka S. 2007. Protein arginine methyltransferases: evolution and assessment of their pharmacological and therapeutic potential. Pharmacol Ther 113:50–87. https://doi.org/10.1016/j.pharmthera.2006.06.007.
10. Deng X, Shao G, Zhang HT, Li C, Zhang D, Cheng L, Elzey BD, Pili R, Ratliff TL, Huang J, Hu CD. 2017. Protein arginine methyltransferase 5 functions as an epigenetic activator of the androgen receptor to promote prostate cancer cell growth. Oncogene 36:1223–1231. https://doi.org/10.1038/onc.2016.287.
11. Gu Z, Li Y, Lee P, Liu T, Wan C, Wang Z. 2012. Protein arginine methyltransferase 5 functions in opposite ways in the cytoplasm and nucleus of prostate cancer cells. PLoS One 7:e44033. https://doi.org/10.1371/journal.pone.0044033.
12. Yu Z, Chen T, Hebert J, Li E, Richard S. 2009. A mouse PRMT1 null allele defines an essential role for arginine methylation in genome maintenance and cell proliferation. Mol Cell Biol 29:2982–2996. https://doi.org/10.1128/MCB.00042-09.
13. Gkountela S, Li Z, Chin CJ, Lee SA, Clark AT. 2014. PRMT5 is required for human embryonic stem cell proliferation but not pluripotency. Stem Cell Rev Rep 10:230–239. https://doi.org/10.1007/s12015-013-9490-z.
14. Yang Y, Bedford MT. 2013. Protein arginine methyltransferases and cancer. Nat Rev Cancer 13:37–50. https://doi.org/10.1038/nrc3409.
15. Elakoum R, Gauchotte G, Oussalah A, Wissler MP, Clement-Duchene C, Vignaud JM, Gueant JL, Namour F. 2014. CARM1 and PRMT1 are dysregulated in lung cancer without hierarchical features. Biochimie 97:210–218. https://doi.org/10.1016/j.biochi.2013.10.021.
16. Hsu JM, Chen CT, Chou CK, Kuo HP, Li LY, Lin CY, Lee HJ, Wang YN, Liu M, Liao HW, Shi B, Lai CC, Bedford MT, Tsai CH, Hung MC. 2011. Crosstalk between Arg 1175 methylation and Tyr 1173 phosphorylation negatively modulates EGFR-mediated ERK activation. Nat Cell Biol 13:174–181. https://doi.org/10.1038/ncb2158.
17. Thandapani P, Song J, Gandin V, Cai Y, Rouleau SG, Garant JM, Boisvert FM, Yu Z, Perreault JP, Topisirovic I, Richard S. 2015. Aven recognition of RNA G-quadruplexes regulates translation of the mixed lineage leukemia protooncogenes. Elife 4:e06234. https://doi.org/10.7554/eLife.06234.
18. Gu Z, Gao S, Zhang F, Wang Z, Ma W, Davis RE, Wang Z. 2012. Protein arginine methyltransferase 5 is essential for growth of lung cancer cells. Biochem J 446:235–241. https://doi.org/10.1042/BJ20120768.
19. Hu H, Qian K, Ho MC, Zheng YG. 2016. Small molecule inhibitors of protein arginine methyltransferases. Expert Opin Invest Drugs 25:335–358. https://doi.org/10.1517/13543784.2016.1144747.
20. Kaniskan H, Jin J. 2017. Recent progress in developing selective inhibitors of protein methyltransferases. Curr Opin Chem Biol 39:100–108. https://doi.org/10.1016/j.cbpa.2017.06.013.
21. Kong GM, Yu M, Gu Z, Chen Z, Xu RM, O'Bryant D, Wang Z. 2017. Selective small-chemical inhibitors of protein arginine methyltransferase 5 with anti-lung cancer activity. PLoS One 12:e0181601. https://doi.org/10.1371/journal.pone.0181601.
22. O'Bryant D, Wang Z. 2018. The essential role of WD repeat domain 77 in prostate tumor initiation induced by Pten loss. Oncogene 37:4151–4163. https://doi.org/10.1038/s41388-018-0254-8.
23. Grypari IM, Logotheti S, Zolota V, Troncoso P, Efstathiou E, Bravou V, Melachrinou M, Logothetis C, Tzelepi V. 2021. The protein arginine methyltransferases (PRMTs) PRMT1 and CARM1 as candidate epigenetic drivers in prostate cancer progression. Medicine (Baltimore) 100:e27094. https://doi.org/10.1097/MD.0000000000027094.

24. Kräutler B. 2008. Chlorophyll breakdown and chlorophyll catabolites in leaves and fruit. Photochem Photobiol Sci 7:1114–1120. https://doi.org/10.1039/b802356p.

25. Hörtensteiner S, Kräutler B. 2011. Chlorophyll breakdown in higher plants. Biochim Biophys Acta 1807:977–988. https://doi.org/10.1016/j.bbabio.2010.12.007.

26. Saide A, Lauritano C, Ianora A. 2020. Pheophorbide a: state of the art. Mar Drugs 18:257. https://doi.org/10.3390/md18050257.

27. Mansoori B, Mohammadi A, Doustvandi MA, Mohammadnejad F, Kamari F, Gjerstorff MF, Baradaran B, Hamblin MR. 2019. Photodynamic therapy for cancer: role of natural products. Photodiagnosis Photodyn Ther 26:395–404. https://doi.org/10.1016/j.pdpdt.2019.04.033.

28. Dailey HA, Dailey TA, Gerdes S, Jahn D, Jahn M, O'Brian MR, Warren MJ. 2017. Prokaryotic heme biosynthesis: multiple pathways to a common essential product. Microbiol Mol Biol Rev 81:e00048-16. https://doi.org/10.1128/MMBR.00048-16.

29. Iida K, Mimura I, Kajiwara M. 2002. Evaluation of two biosynthetic pathways to delta-aminolevulinic acid in *Euglena gracilis*. Eur J Biochem 269:291–297. https://doi.org/10.1046/j.0014-2956.2001.02651.x.

30. Cui BC, Yoon I, Li JZ, Lee WK, Shim YK. 2014. Synthesis and characterization of novel purpurinimides as photosensitizers for photodynamic therapy. Int J Mol Sci 15:8091–8105. https://doi.org/10.3390/ijms15058091.

31. Cho M, Park GM, Kim SN, Amna T, Lee S, Shin WS. 2014. Glioblastoma-specific anticancer activity of Pheophorbide a from the edible red seaweed *Grateloupia elliptica*. J Microbiol Biotechnol 24:346–353. https://doi.org/10.4014/jmb.1308.08090.

32. Larkin RM. 2016. Tetrapyrrole signaling in plants. Front Plant Sci 7:1586. https://doi.org/10.3389/fpls.2016.01586.

33. Hosohata K, Li P, Hosohata Y, Qin J, Roeder RG, Wang Z. 2003. Purification and identification of a novel complex which is involved in androgen receptor-dependent transcription. Mol Cell Biol 23:7019–7029. https://doi.org/10.1128/MCB.23.19.7019-7029.2003.

34. Trott O, Olson AJ. 2010. AutoDock Vina: improving the speed and accuracy of docking with a new scoring function, efficient optimization, and multithreading. J Comput Chem 31:455–461. https://doi.org/10.1002/jcc.21334.

35. Gomes A, Neves M, Cavaleiro JAS. 2018. Cancer, photodynamic therapy and porphyrin-type derivatives. An Acad Bras Cienc 90:993–1026. https://doi.org/10.1590/0001-3765201820170811.

36. Martinez De Pinillos Bayona A, Mroz P, Thunshelle C, Hamblin MR. 2017. Design features for optimization of tetrapyrrole macrocycles as antimicrobial and anticancer photosensitizers. Chem Biol Drug Des 89:192–206. https://doi.org/10.1111/cbdd.12792.

37. Santos EH, Carvalho C, Terzi CM, Nakagaki S. 2018. Recent advances in catalyzed sequential reactions and the potential use of tetrapyrrolic macrocycles as catalysts. Molecules 23:2796. https://doi.org/10.3390/molecules23112796.

38. Kaniskan H, Szewczyk MM, Yu Z, Eram MS, Yang X, Schmidt K, Luo X, Dai M, He F, Zang I, Lin Y, Kennedy S, Li F, Dobrovetsky E, Dong A, Smil D, Min SJ, Landon M, Lin-Jones J, Huang XP, Roth BL, Schapira M, Atadja P, Barsyte-Lovejoy D, Arrowsmith CH, Brown PJ, Zhao K, Jin J, Vedadi M. 2015. A potent, selective and cell-active allosteric inhibitor of protein arginine methyltransferase 3 (PRMT3). Angew Chem Int Ed Engl 54:5166–5170. https://doi.org/10.1002/anie.201412154.

39. Liu F, Zhao X, Perna F, Wang L, Koppikar P, Abdel-Wahab O, Harr MW, Levine RL, Xu H, Tefferi A, Deblasio A, Hatlen M, Menendez S, Nimer SD. 2011. JAK2V617F-mediated phosphorylation of PRMT5 downregulates its methyltransferase activity and promotes myeloproliferation. Cancer Cell 19:283–294. https://doi.org/10.1016/j.ccr.2010.12.020.

40. Hsu W-J, Chen C-H, Chang Y-C, Cheng C-H, Tsai Y-H, Lin C-W. 2021. PRMT1 confers resistance to olaparib via modulating MYC signaling in triple-negative breast cancer. Jpm 11:1009. https://doi.org/10.3390/jpm11101009.

41. Wang J, Wang C, Xu P, Li X, Lu Y, Jin D, Yin X, Jiang H, Huang J, Xiong H, Ye F, Jin J, Chen Y, Xie Y, Chen Z, Ding H, Zhang H, Liu R, Jiang H, Chen K, Yao Z, Luo C, Huang Y, Zhang Y, Zhang J. 2021. PRMT1 is a novel molecular therapeutic target for clear cell renal cell carcinoma. Theranostics 11:5387–5403. https://doi.org/10.7150/thno.42345.

42. Di Lorenzo A, Bedford MT. 2011. Histone arginine methylation. FEBS Lett 585:2024–2031. https://doi.org/10.1016/j.febslet.2010.11.010.

43. Stopa N, Krebs JE, Shechter D. 2015. The PRMT5 arginine methyltransferase: many roles in development, cancer and beyond. Cell Mol Life Sci 72:2041–2059. https://doi.org/10.1007/s00018-015-1847-9.

44. Karkhanis V, Hu YJ, Baiocchi RA, Imbalzano AN, Sif S. 2011. Versatility of PRMT5-induced methylation in growth control and development. Trends Biochem Sci 36:633–641. https://doi.org/10.1016/j.tibs.2011.09.001.

45. Alinari L, Mahasenan KV, Yan F, Karkhanis V, Chung JH, Smith EM, Quinion C, Smith PL, Kim L, Patton JT, Lapalombella R, Yu B, Wu Y, Roy S, De Leo A, Pileri S, Agostinelli C, Ayers L, Bradner JE, Chen-Kiang S, Elemento O, Motiwala T, Majumder S, Byrd JC, Jacob S, Sif S, Li C, Baiocchi RA. 2015. Selective inhibition of protein arginine methyltransferase 5 blocks initiation and maintenance of B-cell transformation. Blood 125:2530–2543. https://doi.org/10.1182/blood-2014-12-619783.

46. Tarighat SS, Santhanam R, Frankhouser D, Radomska HS, Lai H, Anghelina M, Wang H, Huang X, Alinari L, Walker A, Caligiuri MA, Croce CM, Li L, Garzon R, Li C, Baiocchi RA, Marcucci G. 2016. The dual epigenetic role of PRMT5 in acute myeloid leukemia: gene activation and repression via histone arginine methylation. Leukemia 30:789–799. https://doi.org/10.1038/leu.2015.308.

47. Chan-Penebre E, Kuplast KG, Majer CR, Boriack-Sjodin PA, Wigle TJ, Johnston LD, Rioux N, Munchhof MJ, Jin L, Jacques SL, West KA, Lingaraj T, Stickland K, Ribich SA, Raimondi A, Scott MP, Waters NJ, Pollock RM, Smith JJ, Barbash O, Pappalardi M, Ho TF, Nurse K, Oza KP, Gallagher KT, Kruger R, Moyer MP, Copeland RA, Chesworth R, Duncan KW. 2015. A selective inhibitor of PRMT5 with in vivo and in vitro potency in MCL models. Nat Chem Biol 11:432–437. https://doi.org/10.1038/nchembio.1810.

48. Gu Z, Zhou L, Gao S, Wang Z. 2011. Nuclear transport signals control cellular localization and function of androgen receptor cofactor p44/WDR77. PLoS One 6:e22395. https://doi.org/10.1371/journal.pone.0022395.

49. Smil D, Eram MS, Li F, Kennedy S, Szewczyk MM, Brown PJ, Barsyte-Lovejoy D, Arrowsmith CH, Vedadi M, Schapira M. 2015. Discovery of a dual PRMT5-PRMT7 inhibitor. ACS Med Chem Lett 6:408–412. https://doi.org/10.1021/ml500467h.

50. Gao G, Zhang L, Villarreal OD, He W, Su D, Bedford E, Moh P, Shen J, Shi X, Bedford MT, Xu H. 2019. PRMT1 loss sensitizes cells to PRMT5 inhibition. Nucleic Acids Res 47:5038–5048. https://doi.org/10.1093/nar/gkz200.

51. Suzuki S, Kassell NF, Lee KS. 1995. Hemin activation of an inducible isoform of nitric oxide synthase in vascular smooth-muscle cells. J Neurosurg 83:862–866. https://doi.org/10.3171/jns.1995.83.5.0862.